Check for updates

Ocean deoxygenation dampens resistance of diatoms to ocean acidification in darkness

Jia-Zhen Sun[1,2,3], Di Zhang[4], Xiangqi Yi[5], John Beardall[6] and Kunshan Gao[1,2]*

[1]State Key Laboratory of Marine Environmental Science, College of Ocean and Earth Sciences, Xiamen University, Xiamen, China, [2]Co-Innovation Center of Jiangsu Marine Bio-industry Technology, Jiangsu Ocean University, Lianyungang, China, [3]National Biopesticide Engineering Research Centre, Hubei Biopesticide Engineering Research Centre, Hubei Academy of Agricultural Sciences, Wuhan, China, [4]School of Ocean, Yantai University, Yantai, China, [5]Polar and Marine Research Institute, College of Harbor and Coastal Engineering, Jimei University, Xiamen, China, [6]School of Biological Sciences, Monash University, Clayton, VIC, Australia

Respiratory activity in the oceans is declining due to the expansion of hypoxic zones and progressive deoxygenation, posing threats to marine organisms along with impacts of concurrent ocean acidification. Therefore, understanding the combined impacts of reduced $p\text{O}_2$ and elevated $p\text{CO}_2$ on marine primary producers is of considerable significance. Here, to simulate diatoms' sinking into the aphotic zone of turbid coastal water, we exposed the diatoms *Thalassiosira pseudonana* and *Thalassiosira weissflogii* in darkness at 20°C to different levels of $p\text{O}_2$ and $p\text{CO}_2$ conditions for ~3 weeks, and monitored their biomass density, photosynthetic activity and dark respiration, and examined their recovery upon subsequent exposure to light at 20°C, simulating surface water conditions. Along with decreased cell abundance and size, measured photosynthetic capacity and dark respiration rates in these two diatoms both gradually decreased during the prolonged darkness. Reduced $p\text{O}_2$ alone did not negatively affect the photosynthetic machinery in both the dark-survived diatom, and enhanced their subsequent recovery upon light exposure. Nevertheless, the combination of the elevated $p\text{CO}_2$ and reduced $p\text{O}_2$ (equivalent to hypoxia) led to the biomass loss by about 90% in *T. pseudonana*, and delayed the recovery of both species upon subsequent exposure to light, though it did not reduce the cell concentration of *T. weissflogii* during the elongated darkness. Our results suggest that reduced O_2 availability diminishes the abilities of the diatoms to cope with the acidic stress associated with ocean acidification, and the expansion of hypoxic waters could delay the photosynthetic recovery of coastal diatoms when they are transported upwards through mixing from dark layers to sunlit waters.

KEYWORDS

ocean deoxygenation, diatom, darkness tolerance, prolonged darkness, seed bank

1 Introduction

Ocean global changes are exposing phytoplankton cells to multiple stressors, including deoxygenation (DeO_2) triggered by warming and eutrophication, and ocean acidification associated with elevated pCO_2 (Gattuso et al., 2015; Gao et al., 2019; Limburg et al., 2020). The decline in the dissolved O_2 (DO) content of coastal seawaters is mainly attributed to the heterotrophic degradation of organic matter that settles out of the euphotic layer, inherently leading to acidification in hypoxic zones (Cai et al., 2011; Gobler and Baumann, 2016; Wang et al., 2017). Over the past 50 years, the oxygen content of the ocean has dropped by 1-7% (Keeling et al., 2010). This decrease has been more rapid and intensive in nearshore waters, resulting in the identification of over 500 hypoxic sites (defined by dissolved $O_2 < 63$ µM) (Diaz and Rosenberg, 2008; Gilbert et al., 2010; Breitburg et al., 2018), with some even extending into the euphotic layer (Ye et al., 2016).

Diatoms, contributing approximately 40% of marine primary production, play a crucial role in the food web and biogeochemical cycles (Duarte et al., 2013), and are particularly dominant along coasts where DeO_2 is most severe (Broman et al., 2017; Wang et al., 2017). During diatom blooms, the depletion of nutrients, particularly silicate, renders the surface layer of the water column inhospitable, leading to a mass sinking of the diatom cells (Bienfang et al., 1982; Smetacek, 1985). Global surveys have revealed that living diatoms associated with fast-sinking mechanisms are widely distributed in the benthos (Agusti et al., 2015) and can survive for months in darkness (Katayama et al., 2015; Kennedy et al., 2019; Mou et al., 2022; Juchem et al., 2023). To maintain viability in prolonged darkness, diatoms and other phytoplankton groups typically reduce their metabolic output by adjusting their physiologies to conserve energy stocks (McMinn and Martin, 2013). In some extreme cases, phytoplankton can exhibit mixotrophy and generate resting spores to withstand harsh environments (McMinn and Martin, 2013; Raven and Beardall, 2022). Beyond sediment burial, the resuspension of settled phytoplankton induced by strong physical forces provides them advantages in shaping community structures and seeding future blooms (Preston et al., 1980; Malone et al., 1983; McQuoid and Godhe, 2004; Mestre and Hofer, 2021). In addition, changes in the concentrations of O_2 and CO_2 with depth have been suggested to influence diatoms' physiology (Gao and Campbell, 2014; Sun et al., 2022). Therefore, investigating the fate of diatoms exposed to changing levels of pO_2 and pCO_2 (pH) during the sinking process is of ecological and physiological significance. During the settling process, diatoms appear to remain in a vegetative state, as the environment in hypoxic water columns is not favorable to spore formation (Kamatani, 1997; Oku and Kamatani, 1999), though diatoms have been reported to use nitrite respiration to form resting spores in dark anoxic conditions (Kamp et al., 2011, 2013), contributing to their dominance in coastal anoxic sediments (Broman et al., 2017). The negligible respiration demands for the minimal oxidative metabolism of phytoplankton (Falkowski and Raven, 1997) suggest that reduced O_2 levels alone may not influence their tolerance to darkness. On the contrary, decreased O_2 availability may benefit phytoplankton by slowing down the

consumption of intracellular energy reserves. On the other hand, it is generally understood that the acidification associated with elevated pCO_2 increases the energy demands to drive H^+ extrusion (Taylor et al., 2012), which has been experimentally shown in diatoms (Wu et al., 2010; Goldman et al., 2017; Qu et al., 2021). Consequently, interactive effects of DeO_2 and acidification are expected, and we hypothesize that the resistance of diatoms to concurrent acid stress with increased pCO_2 may be affected by decreased pO_2, since the availability of the latter impacts respiratory energy generation. By simulating the conditions under which diatoms sink in the darkness of turbid coastal water, we ran dark incubations for approximately 3 weeks with two diatom species, *Thalassiosira pseudonana* and *Thalassiosira weissflogii*, under different pO_2 vs pCO_2 levels, and found that concurrent ocean deoxygenation and acidification synergistically reduced the cell concentration and size of the diatoms in the dark with their respiration being suppressed.

2 Materials and methods

2.1 Dark incubation and recovery experiment

The coastal diatoms *T. pseudonana* (CCMP 1007) and *T. weissflogii* (CCMP 1336) obtained from the Center for Collections of Marine Bacterial and Phytoplankton (Xiamen University) were grown in 0.22 µm-filtered artificial seawater prepared according to the Aquil* medium (Sunda et al., 2005). *T. pseudonana* and *T. weissflogii* are widely chosen as typical organisms for research on phytoplankton physiology and physiological ecology. All chemicals used were purchased from Sinopharm Chemical, and the culture medium and vessels were sterilized by autoclaving (121°C for 20 min).

The experiment was run in prolonged darkness followed by a short period of light exposure (Supplementary Figure S1). Pre-cultures (2 L) were maintained at 20°C and 200 µmol photons $m^{-2} s^{-1}$ (12:12 h light: dark cycle) in a plant growth chamber (HZ100LG, Ruihua, Wuhan, China) without aeration, and were diluted every one or two days with fresh medium to ensure exponential growth. After one week, diatoms were transferred into newly prepared medium (triplicate cultures, 1 L) at the end of photoperiod, and were then maintained in complete darkness for about 3 weeks with continuous aeration (100 mL min^{-1}) at the targeted CO_2 and O_2 concentrations. The initial diatom cell concentrations were about 1.6×10^5 and 1.2×10^4 cells mL^{-1} for *T. pseudonana* and *T. weissflogii*, respectively. The diatoms were maintained under three treatments: (1) outdoor ambient air (AOAC, $O_2 = 217$ µM, $CO_2 = 15$ µM, $pH_T = 8.0$); (2) low O_2 & ambient CO_2 (LOAC, $O_2 = 78$ µM, $CO_2 = 14$ µM, $pH_T = 8.0$); (3) low O_2 & high CO_2 (LOHC, $O_2 = 58$ µM, $CO_2 = 56$ µM, $pH_T = 7.5$). The low O_2 level were around the hypoxic range, and combined levels of low O_2 and high CO_2 were set according to the modelled results for 2100 in coastal waters (Cai et al., 2011). The presented O_2, CO_2, and pH_T values are averages from across the experiment. N_2, CO_2, and air were mixed proportionally to create the distinct and stable $O_2:CO_2$ combinations in the gas stream for aeration.

Recovery experiments from darkness to light were conducted following 516- or 528-hour dark culture. The cells of *T. pseudonana* and *T. weissflogii* were transferred into a 12:12 h cycle (light: dark) for 1 or 3 days, respectively (Supplementary Figure S1), in the cultures (150 mL) maintained at 20°C, 175 µmol photons m^{-2} s^{-1} without aeration.

2.2 Determination of dissolved O_2 and carbonate chemistry parameters

A precise single-channel fiber optic oxygen sensor (Microx 4, PreSence, Germany) was used for measurement of dissolved O_2. The pH was determined with a high-quality pH meter (Orion StarA11, Thermo, USA), calibrated with standard National Bureau of Standards (NBS) buffer solutions (Hanna). Filtered samples (Cellulose Acetate Membranes, 0.45 µM), fixed with saturated $HgCl_2$ (V:V, 1000:1), were stored for total alkalinity (TA) measurement, which was conducted with a TA titrator (AS-ALK+, Apollo, SciTech). CO_2 concentrations and pH_T of the medium were estimated from the corresponding pH_{NBS} and TA using CO2SYS software (Lewis et al., 1999) with the equilibrium constants K_1 and K_2 for carbonic acid dissociation from Millero et al. (2006).

2.3 Measurement of cell concentration, size and pigments content

Cell number and diameter were assessed using a Coulter Particle Count and Size Analyzer (Z2, Backman Coulter, USA). Pigment samples were filtered onto glass-fiber filters (25 mm, Whatman GF/F, USA) under a pressure of 0.01 MPa and stored at -20°C until analysis. Chlorophyll *a* (Chl *a*) and carotenoid concentrations were determined using an ultraviolet spectrophotometer (TU-1810S, Puxi, China) after extraction overnight at 4°C in absolute methanol, and were calculated as described according to Ritchie (2006) and Strickland and Parsons (1968).

2.4 Photosynthetic parameters measurements

Chlorophyll *a* fluorescence characteristics were determined using a Multiple Excitation Wavelength Chlorophyll Fluorescence Analyzer (MULTI-COLOR-PAM, Walz, Germany). Samples were dark adapted for 20 min before the measurements. The minimum fluorescence (F_0) of the sample was measured with a weak probe pulse (~5 µmol photons m^{-2} s^{-1}), and the maximum fluorescence (F_m) was then measured by applying a saturating light pulse of 8000 µmol photons m^{-2} s^{-1} (0.8 s), the maximum quantum yield of photosystem II (PSII) was estimated as:

$$\text{Fv/Fm} = \frac{(F_m - F_0)}{F_m}$$

Rapid light curves for relative electron transport rate (rETR, au) were measured at light intensities (PAR) ranging from 0-2442 µmol

photons m^{-2} s^{-1} and each PAR exposure lasted for 30 s. The parameters were calculated according to Eilers and Peeters (1988):

$$\text{rETR} = \frac{PAR}{a \times PAR^2 + b \times PAR + c}$$

Photosynthetic parameters, including the maximum rETR (rETR_{max}) and the photosynthetic light-harvesting efficiency (α) were calculated as:

$$\text{rETR}_{max} = \frac{1}{b + 2\sqrt{a \times c}}$$

and

$$\alpha = \frac{1}{c}$$

2.5 Determination of mitochondrial respiration

A Clark-type oxygen electrode (Hansatech, UK) was used to measure dark respiration under the culture conditions. The rate of respiration was estimated based on linear O_2 changes in the reaction vessel. Cells were filtered onto polycarbonate membrane filters (1.2 µm, Millipore, Germany) under a pressure of 0.01 MPa and subsequently re-suspended in fresh medium (2 mL) buffered with 20 mM Tris (pH_T = 8.0 for AOAC and LOAC, pH_T = 7.5 for LOHC) to maintain a stable pH during the measurements. The Tris-buffered medium was flushed with pure nitrogen and ambient air to achieve the targeted O_2 levels.

2.6 Statistical analyses

Generalized additive models (GAMs), emphasizing patterns of physiological parameters over time, were constructed using the 'mgcv' package in R to analyze changes in physiology through the dark-phase (Wood, 2017). Linear mixed effects models (LMMs) from 'nlme' package in R were applied when parameters exhibited linear changes over time (Pinheiro and Bates, 2006). Pairwise comparisons between treatments and the control at each time point were conducted using the 'itsadug' package for GAMs or the 'emmeans' package for LMMs, respectively. Model building, selection, and validation followed the principles and guidelines outlined in Pinheiro and Bates (2006); Zuur et al. (2009) and Wood (2017). If necessary, the original data were subjected to a square root (SQRT) transformation. The selected models and corresponding results are provided in Supplementary Tables 1-6. Paired samples *t*-test (two-tailed, $\alpha = 0.05$) was employed to identify differences between values during transitions from dark to light phase or within the light phase.

3 Results

The concentrations of O_2 and CO_2, and pH in the cultures of *T. pseudonana* and *T. weissflogii* were maintained at distinct levels

among the treatments during the 21 or 22-day period of darkness (Supplementary Figure S1). Upon subsequent transfer of the cells to light, concentrations of O_2 and pH increased, while concentrations of CO_2 decreased (Supplementary Figure S1).

3.1 Changes in cell concentration and size

In the initial 12 hours of darkness, *T. pseudonana* and *T. weissflogii* cultivated under ambient O_2 and ambient CO_2 (AOAC) exhibited increases in cell concentrations of approximately 24% and 41%, respectively (Figures 1A,B and inset). Following this, the cell concentrations of AOAC-cultivated *T. pseudonana* gradually decreased, leading to a 57% loss by the end of prolonged darkness, compared to its peak value. In contrast, the cell concentration of AOAC-cultivated *T. weissflogii* remained relatively stable after the initial 12 hours of darkness, culminating in a 49% enhancement compared to the initial value. Based on the generalized additive models (GAMs), reduced O_2 alone (LOAC) affected the temporal patterns of cell concentrations in *T. pseudonana* and *T. weissflogii* (Wald tests, $p \leq 0.0339$, detailed p values are provided in Supplementary Tables 3 and 4), which was supported by the pairwise comparisons (Supplementary Figure S2A,B). However, at the end of prolonged darkness, the combination of reduced O_2 and elevated CO_2 (LOHC) exacerbated the decline of cell concentration in *T. pseudonana* to 90%. Meanwhile, LOHC led to a 61% increase in *T. weissflogii*,

which was less than the enhancement achieved through reduced O_2 alone (71%).

After one cycle of re-illumination, significant increases in cell concentrations were exclusively observed in the diatoms grown under LOAC conditions (Figures 1A,B, Paired samples t-test, $p = 0.0135, 0.0322$). In contrast, LOHC-cultivated *T. weissflogii* failed to achieve any increase in cell concentration even after three cycles of re-illumination (Paired samples t-test, $p = 0.0847$), while AOAC- and LOAC-cultivated *T. weissflogii* increased their cell concentrations by 141% and 246%, respectively.

The cell diameters of both diatoms grown and surviving under different pO_2/pCO_2 levels sharply decreased over time during the extended period of darkness (Figures 1C,D). The cell diameter of *T. pseudonana* exhibited a short increase between the 12 and 24 hours of darkness and then decreased, culminating in 10%-12% decrease, compared to their peak values. In contrast, the cell diameters of *T. weissflogii* remained relatively stable after the initial decrease, ultimately reducing by 6%-9%. Although LOAC and LOHC affected the temporal pattern of cell diameters of both diatoms (Wald tests, $p = <0.0001-0.4520$), the impacts were relatively small (Supplementary Figure S2C,D). After one cycle of illumination, significant increases in cell diameters were observed in the diatoms grown under AOAC and LOAC conditions, with the latter showing better recovery (Figures 1C,D, Paired samples t-test, $p = 0.0009-0.0446$). However, LOHC-grown *T. weissflogii* failed to achieve increases in cell diameter even after three cycles of re-illumination (Paired samples t-test, $p = 0.1293$), while AOAC-
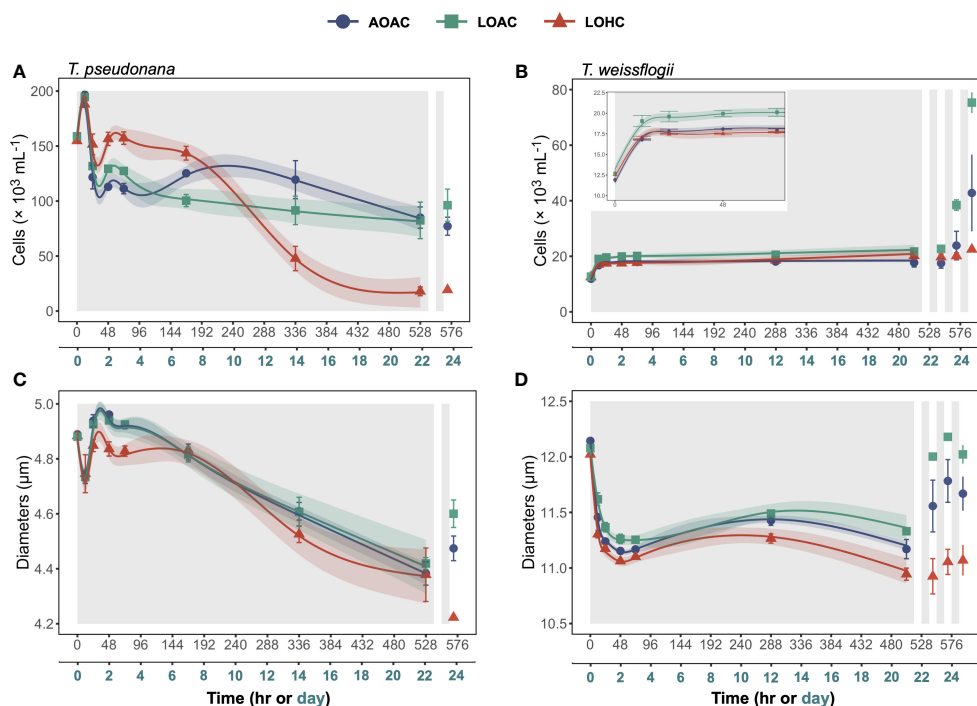

FIGURE 1
Changes in cell concentrations **(A, B)** and diameters **(C, D)** of *Thalassiosira pseudonana*, and *Thalassiosira weissflogii* over time in prolonged darkness under different levels of O_2 and CO_2. AOAC ($O_2 = 217$ μM, $CO_2 = 15$ μM), LOAC ($O_2 = 78$ μM, $CO_2 = 14$ μM) and LOHC ($O_2 = 58$ μM, $CO_2 = 56$ μM) represent different treatments (indicated as different colors) during the dark period (the gray shaded parts), and the following white intervals between the grays represent the light phase (12 h, 175 μmol photons m^{-2} s^{-1}). Data are the means $\pm$ SD, solid lines and shadows are predicted values from GAMs with 95% confidence intervals (n = 3 independent bottles).

and LOAC-cultivated *T. weissflogii* increased their cell diameters by 4% and 6%, respectively (Paired samples *t*-test, *p* = 0.0362, 0.0029).

3.2 Changes in photosynthetic pigments

The temporal patterns of chlorophyll *a* (Chl *a*) concentrations per volume of culture in *T. weissflogii* mirrored cell concentrations, whereas those in *T. pseudonana* remained stable throughout the period of darkness (Supplementary Figures S3A,B). During the prolonged darkness, the changes in carotenoid concentrations of these two diatoms were negligible (Supplementary Figures S3C,D). After one cycle of re-illumination, both Chl *a* and carotenoid concentrations in *T. pseudonana* cultures significantly decreased (Paired samples *t*-test, *p* = 0.0210-0.0370, 0.0228-0.0304). Only *T. weissflogii* cultivated under the LOAC condition demonstrated a significant increase in Chl *a* and carotenoid concentrations per

volume of culture after three-cycles of re-illumination by 328% and 62%, respectively (Paired samples *t*-test, *p* = 0.0004, 0.0133).

Both the cellular Chl *a* and carotenoid contents of AOAC-cultivated *T. pseudonana* declined during the initial 12 hours of darkness, followed by an increase and subsequent stabilization (Figures 2A,C and insets). Notably, *T. pseudonana* cultured under LOHC conditions showed dramatic increases in cellular photosynthetic pigment content. By applying the linear mixed-effects models (LMMs) with data collected from 0-168 hours of darkness, it appeared that the effects of reduced O_2 alone on contents of both photosynthetic pigments were time dependent (Wald tests, *p* < 0.0001, detailed *p* vales are provided in Supplementary Table 5), with negative effects observed at 72 hours of darkness while positive effects were apparent at 168 hours (Supplementary Figures S4A,C). However, under elevated CO_2 level, the promoting effects of reduced O_2 on cellular Chl *a* and carotenoid contents turned into neutral and negative impacts,
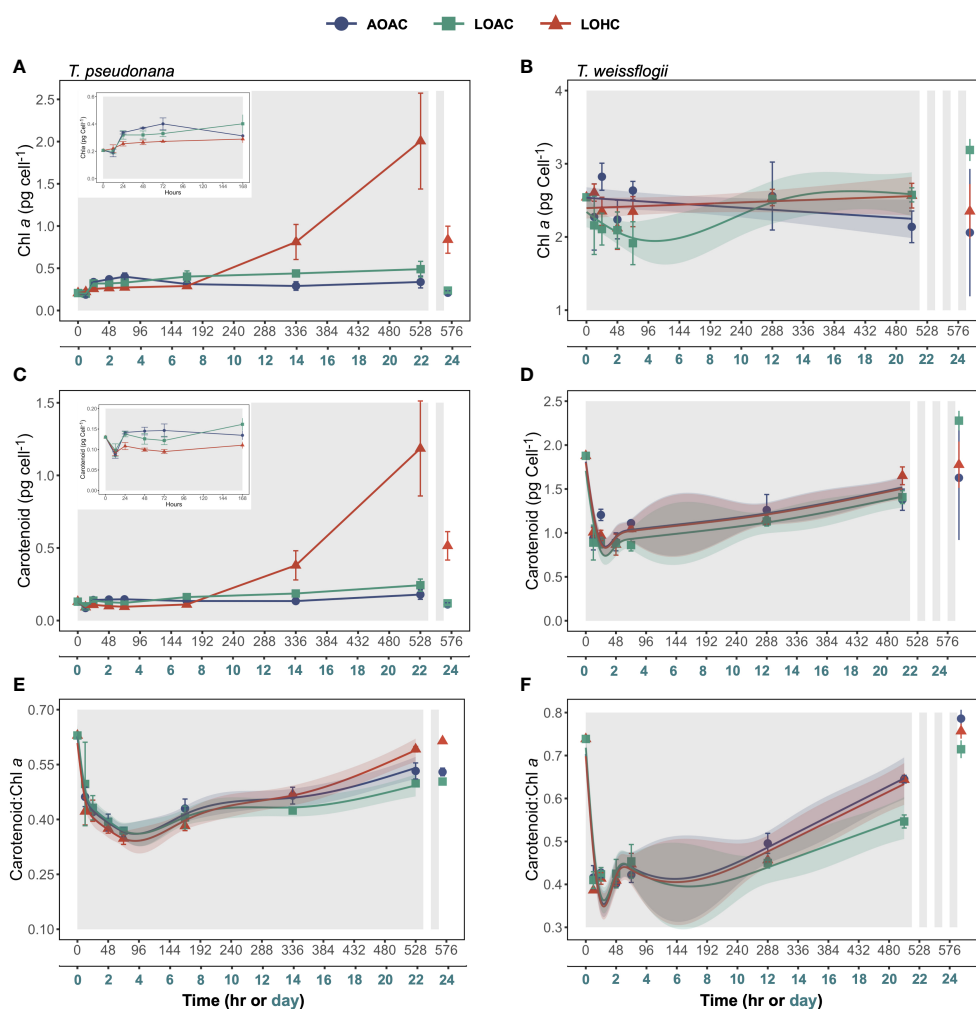

FIGURE 2
Changes in cellular chlorophyll *a* (Chl *a*) contents **(A, B)**, Carotenoid contents **(C, D)** and Carotenoid: Chl *a* ratio **(E, F)** of *Thalassiosira pseudonana*, and *Thalassiosira weissflogii* over time in prolonged darkness under different levels of O_2 and CO_2. AOAC (O_2 = 217 µM, CO_2 = 15 µM), LOAC (O_2 = 78 µM, CO_2 = 14 µM) and LOHC (O_2 = 58 µM, CO_2 = 56 µM) represent different treatments (indicated as different colors) during the dark period (the gray shaded parts), and the following white intervals between the grays represent the light phase (12 h, 175 µmol photons m^{-2} s^{-1}). Data are the means $\pm$ SD, solid lines and shadows are predicted values from GAMs with 95% confidence intervals (n = 3 independent bottles).

respectively (Supplementary Figures S4A,C). The cellular contents of Chl *a* in AOAC-cultivated *T. weissflogii* gradually decreased throughout the prolonged darkness, culminating in a 24% reduction compared to its peak value. While *T. weissflogii* cellular carotenoid content decreased sharply when first under darkness, it then gradually increased (Figures 2B,D). Although the GAMs analysis indicated that LOAC influenced the temporal patterns of cellular Chl *a* content in *T. weissflogii* (Wald tests, *p* = 0.0030), the effect of LOAC was significant only in the early stages of prolonged darkness (negative) (Supplementary Figure S4B). In contrast, LOHC showed no effects on both photosynthetic pigment contents (Supplementary Figures S4B,D). Both the cellular Chl *a* and carotenoid contents of *T. pseudonana* under different pO_2/pCO_2 levels decreased after one cycle of re-illumination (Paired samples *t*-test, *p* = 0.0430-0.0912, 0.0338-0.0955), and only LOAC-cultivated *T. weissflogii* increased their cellular pigment contents after three cycles of recovery (Paired samples *t*-test, *p*< 0.0001, 0.0132).

The carotenoid: Chl *a* ratio in *T. pseudonana* and *T. weissflogii* cultured under AOAC condition sharply decreased when the diatoms entered darkness, then gradually increased (Figures 2E,F). Particularly for *T. weissflogii*, the carotenoid: Chl *a* ratio decreased by 44%-48% within 12 hours of darkness. Reduced O_2 alone significantly influenced the temporal patterns of carotenoid: Chl *a* ratio in both diatoms (Wald tests, *p* ≤ 0.0239), with the negative effects exacerbated with time (Supplementary Figures S4E,F). However, when combined with elevated CO_2, the negative effects from reduced O_2 on carotenoid: Chl *a* ratio diminished, even turning positive in *T. pseudonana* at the end of prolonged darkness (Supplementary Figures S4E, F). One cycle of re-illumination had little effect on the carotenoid: Chl *a* ratio of *T. pseudonana* (Paired samples *t*-test, *p* = 0.0074 -0.7864), and after three cycles of recovery, carotenoid: Chl *a* ratio of *T. weissflogii* increased by 18%-31%, approaching to their initial values (Figures 2E, F, Paired samples *t*-test, *p* = 0.0013-0.0099).

3.3 Changes in photosynthetic parameters

The maximum quantum yield of photosystem II (Fv/Fm) in AOAC-grown diatoms exhibited minor fluctuations throughout the prolonged darkness (~0.59-0.70 for *T. pseudonana* and 0.69- 0.74 for *T. weissflogii*) (Figures 3A,B). Reduced O_2 alone showed no impact on Fv/Fm of *T. pseudonana* (Wald tests, *p* = 0.2170), while its combination with elevated CO_2 led to a significant decrease (around 37%) in Fv/Fm after approximately 288 hours of darkness (Supplementary Figure S5A, Wald tests, *p*< 0.0001). Although the effects of reduced O_2 under different CO_2 levels on *T. weissflogii* were time-dependent (Wald tests, *p*< 0.0001, detailed *p* values are provided in Supplementary Table 6), no significant difference at most time points was observed (Supplementary Figure S5B). Upon re-illumination, the Fv/Fm of both diatoms declined, with cells grown under LOHC showing the most decrease, 23% for *T. pseudonana* and 42% for *T. weissflogii*, respectively (Figures 3A,B, Paired samples *t*-test, *p* = 0.0004-0.0067).

Rapid light curves were employed to determine changes in photosynthetic capacity of diatoms over time during prolonged darkness and re-illumination (Supplementary Figures S6 and Supplementary Figure S7). The maximum rETR (rETR$_{max}$) and the photosynthetic light-harvesting efficiency (α) of AOAC-cultivated *T. pseudonana* initially increased at the onset of darkness, followed by a decrease, culminating in a 74% and 42% decline compared to their peak values, respectively (Figures 3C,E). Reduced O_2 alone did not impact the rETR$_{max}$ of *T. pseudonana*, while it altered the temporal pattern of α, with the negative impacts enhanced over time (Supplementary Figure S5C,E, Wald test, *p* = 0.0040). When coupled with elevated CO_2, reduced O_2 initially positively affected rETR$_{max}$ and α but, after about 192 hours of darkness, it turned into negative (Supplementary Figure S5C,E, Wald test, *p* ≤ 0.0001), resulting in a 48% and a 46% decline compared to the control, respectively, at the end of prolonged darkness. The temporal pattern of rETR$_{max}$ in *T. weissflogii*, cultivated under AOAC condition, mirrored that of *T. pseudonana*, while its α declined during the initial 24-hour darkness and then stabilized (Figure 3D,F). Reduced O_2 alone affected the temporal patterns of rETR$_{max}$ and α of *T. weissflogii* (Wald test, *p* ≤ 0.00293), with the negative impacts gradually turning positive (Supplementary Figure S5D,F). Notably, when combined with elevated CO_2, reduced O_2 initially showed a positive impact on both rETR$_{max}$ and α, then effects turned negative and neutral, respectively (Wald test, *p* ≤ 0.0010, Supplementary Figure S5D,F), resulting in a 28% reduction in rETR$_{max}$ compared with the control. Once again, the diatoms cultivated under LOHC condition exhibited the slowest recovery in photosynthetic activity upon light exposure, (Figures 3C–F).

3.4 Changes in dark respiration

The dark respiration rates of these two diatoms gradually decreased by about 19%-46% within the initial 48-72 hours of darkness and then remained relatively stable thereafter (Figure 4). The reduced O_2 level, under both CO_2 concentrations, had significant effects on dark respiration rates of both diatoms, and these effects varied with time (Supplementary Figure S8, Wald tests, *p* ≤ 0.0002). This was more evident for *T. pseudonana*, whose respiration rates were significantly inhibited only in the first 24 hours of darkness, while those of *T. weissflogii* were significantly reduced throughout the darkness (Supplementary Figure S8). Although elevated CO_2 did not exhibit additional impacts under the reduced O_2 conditions, it appeared to diminish the negative impacts on dark respiration rate in *T. pseudonana* (Supplementary Figure S8A).

4 Discussion

While the typical coastal diatoms *T. pseudonana* and *T. weissflogii* could survive 3 weeks in darkness, with the former showing greater vulnerability (Figure 1), reduced levels of O_2 and pH exacerbated the biomass decline, especially in the smaller species, *T. pseudonana*.

Diatoms and other phototrophs typically experience diminished photosynthetic performance in response to prolonged
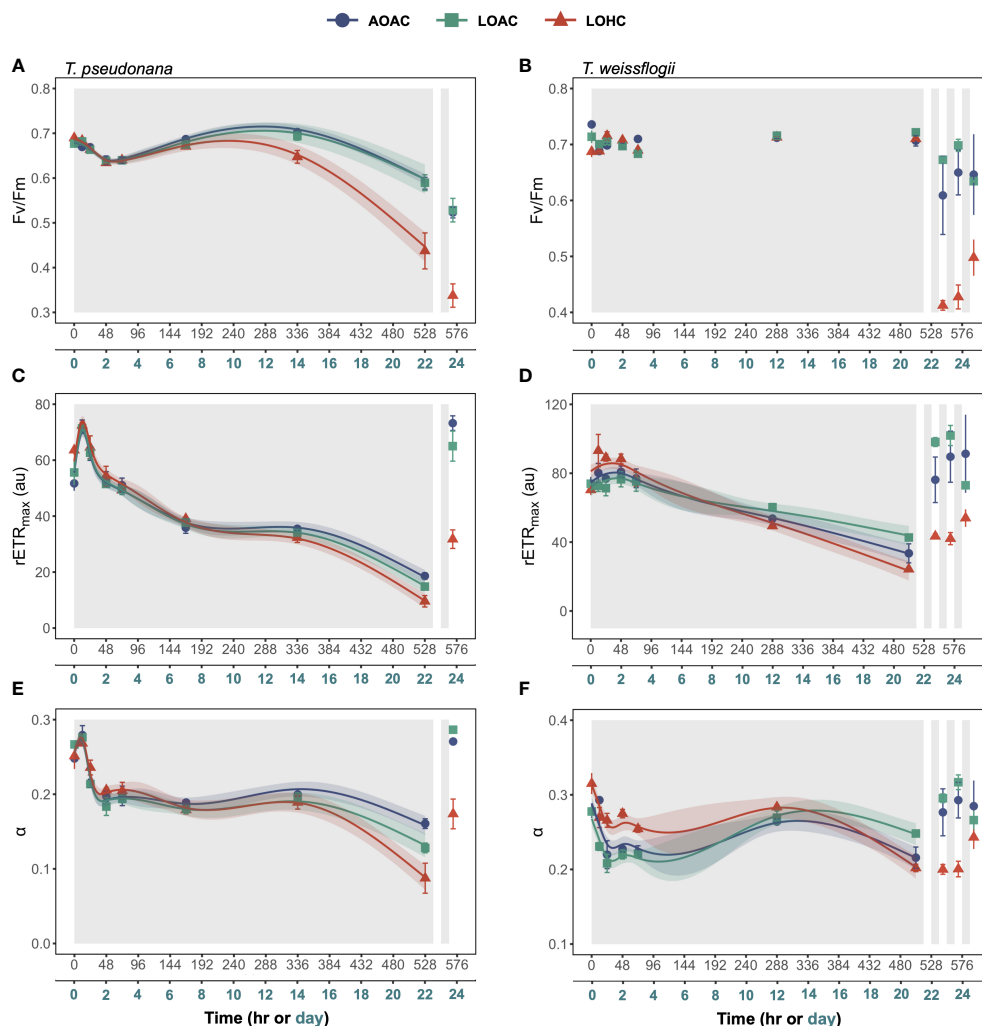
FIGURE 3

Changes in Fv/Fm **(A, B)**, rETR maximum (rETR$_{max}$) **(C, D)** and the photosynthetic light-harvesting efficiency (α) **(E, F)** of *Thalassiosira pseudonana*, and *Thalassiosira weissflogii* over time in prolonged darkness under different levels of O_2 and CO_2. AOAC (O_2 = 217 μM, CO_2 = 15 μM), LOAC (O_2 = 78 μM, CO_2 = 14 μM) and LOHC (O_2 = 58 μM, CO_2 = 56 μM) represent different treatments (indicated as different colors) during the dark period (the gray shaded parts), and the following white intervals between the grays represent the light phase (12 h, 175 μmol photons m^{-2} s^{-1}). Data are the means $\pm$ SD, solid lines and shadows are predicted values from GAMs with 95% confidence intervals (n = 3 independent bottles).

darkness in cold environments (Jochem, 1999; McMinn and Martin, 2013), along with downregulation of molecular processes involved in the photosynthetic machinery, as in the polar diatom *Fragilariopsis cylindrus* (Mock et al., 2017; Kennedy et al., 2019). In the present work, we also observed that the photosynthetic electron transport capacity, measured as rETR$_{max}$ and α, of both diatoms, declined with time during the elongated darkness at 20 °C (Figure 3), which is consistent with studies in the temperate diatom *Phaeodactylum tricornutum* (Nymark et al., 2013; Bai et al., 2016). However, maximum quantum yield (F$_v$/F$_m$) remained high, except for *T. pseudonana* at the end of the elongated darkness. This correlates with the changes in cellular Chl *a* content, which after an initial drop during the first 12 hours of dark incubation remained fairly steady (Figures 2 and 3). An exception was found in *T. pseudonana* exposed to LOHC conditions, where the cellular Chl *a* content rose strongly in the latter phase of the prolonged darkness, which correlated with the

marked decrease in cell concentration of this species (Figure 1). Although the degradation of *in vitro* photosynthetic pigments has previously been shown to slow down under darkness and reduced O_2 availability (Lee et al., 2014), our measurements did not distinguish between living and dead diatom cells, therefore the measured changes in the pigment content could only reflect that in the culture (i.e. that in dead as well as living cells in the medium). Discrepancies observed between cell and Chl *a* concentrations per volume of culture of *T. pseudonana* (Figures 1 and Supplementary Figure S3) in the later darkness period prompt caution in interpreting changes of biomass and quantum efficiency of PSII. Franklin et al. (2009) showed that in a number of microalgae (including *T. pseudonana*) the relationship between effective quantum yield (Fv'/Fm') and the viability of cells was non-linear, with only minor declines (< 10%) in this parameter with up to ~50% dead cells in the culture. Based on the relationship between the proportion of dead cells and PS II efficiency of *T. pseudonana*
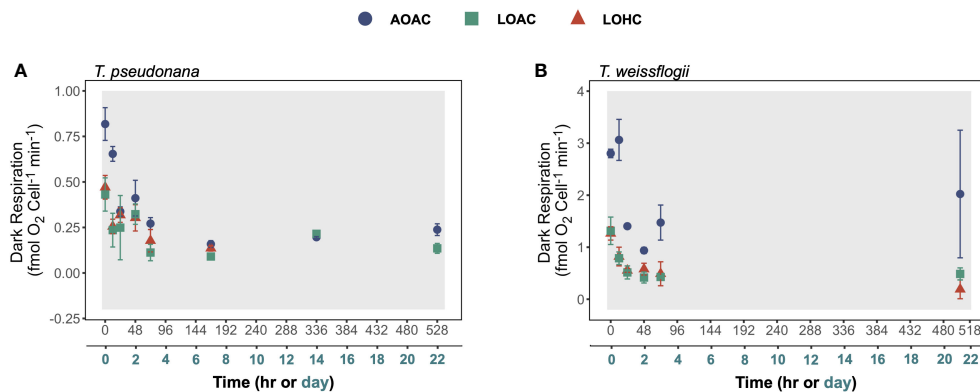
FIGURE 4

Changes in dark respiration of *Thalassiosira pseudonana* **(A)**, and *Thalassiosira weissflogii* **(B)** over time in prolonged darkness under different levels of O_2 and CO_2. AOAC (O_2 = 217 µM, CO_2 = 15 µM), LOAC (O_2 = 78 µM, CO_2 = 14 µM) and LOHC (O_2 = 58 µM, CO_2 = 56 µM) represent different treatments (indicated as different colors) during the dark period (the gray shaded parts), and the following white intervals between the grays represent the light phase (12 h, 175 µmol photons m^{-2} s^{-1}). Due to the dramatically loss in *T. pseudonana* after 168 hours of darkness, their respiration rate was not measured to avoid imprecise. Data are the means $\pm$ SD (n = 3 independent bottles).

(Franklin et al., 2009), the decrease in Fv/Fm by about 37% suggests a loss of about 60%-90% of biomass under LOHC. This aligns with our measured decline (88%) based on cell concentrations, suggesting that *T. pseudonana* exhibits limited resilience to darkness (Figure 1). The presence of broken cells trapped by GF/F membrane may affect the accuracy of Chl *a* concentration as a biomass indicator. Nevertheless, since the carotenoid: Chl *a* ratio of the two diatoms rose after prolonged darkness, an enhancement in antioxidant capacity could be expected (Katayama et al., 2011).

The consumption of stored energy reserves is an evolutionary adaptation of phytoplankton to periodic and stochastic events (Falkowski and Raven, 1997), influencing darkness tolerance (Jochem, 1999; Schaub et al., 2017). It is well-established that phytoplankton respiration decreases during prolonged darkness, whether the cells are vegetative or resting (Anderson, 1976; Peters, 1996; Kennedy et al., 2019). However, persistent consumption may ultimately lead to population collapse, as evidenced by increased mortality rates of *Scenedesmus acuminatus* when intracellular carbon content reached a certain point (Dehning and Tilzer, 1989). Assuming a ratio of consumed O_2 to organic carbon as 6:1, which is based on the reaction of aerobic respiration that uses glucose as the substrate, the estimated consumption of *T. pseudonana* in this work ranged from 0.63-1.16 pmol per cell throughout the whole prolonged darkness. This constitutes 45%-82% of the reported intracellular organic contents, a larger proportion compared to the consumption of *T. weissflogii*, which accounts for only 11%-37% (Hong et al., 2017; Li et al., 2018; Sun et al., 2022). The difference in intracellular organic carbon consumption is likely a key factor contributing to the observed greater darkness tolerance observed in *T. weissflogii* compared to *T. pseudonana* in this study (Figure 1). Diatoms have also been suggested to actively uptake organic carbon compounds such as amino acids and fatty acids from the medium (Price and Harrison, 1988; McMinn and Martin, 2013); such processes might have influenced the survival of the diatoms during the elongated darkness in this experiment.

The minimal oxidative metabolism required for sustaining phytoplankton viability is virtually negligible, achievable at nanomolar O_2 levels (Falkowski and Raven, 1997; Wong et al., 2023). Consequently, diatoms should be able to adjust their respiratory cost by constraining respiration. The reduced O_2 availability aided in such adjustment. On the other hand, elevated pCO$_2$ associated with the acidic stress is known to enhance respiration rate of diatoms to accommodate the increased energy demands involved in maintaining intracellular pH homeostasis (Wu et al., 2010; Goldman et al., 2017; Qu et al., 2021; Gao et al., 2022). However, a recent study suggests that the increased respiration may not be sufficient to counteract the negative effects induced by acidic stress in darkness, as the cell growth rate of the diatom *P. tricornutum* decreased in a 48-hour period of complete darkness (Qu et al., 2021). Thus, the diminished energy supply resulting from reduced O_2 availability may further weaken the ability of the diatoms to withstand acidic stress, leading to intensified biomass loss in *T. pseudonana* and delayed the recovery of both diatoms upon subsequent exposure to light in our experiment (Figure 1). Diatoms are renowned for their capability to form a resting stage in stressful environments, such as nutrient depletion and cold temperature (Chen et al., 2014; Ma et al., 2020; Wang et al., 2024). However, considering the relatively shorter duration of darkness and the milder stressors applied in our experiment, during the elongated darkness along with lowered levels of O_2 and pH, the majority of the cells appeared to be in a vegetative state with minimal physiological activity. This is supported by the fact that the cells retained some photosynthetic ability even at the end of the dark exposure (Figure 3).

It should be noted that our results are only relevant to coastal hypoxic waters, since we did not set the temperature as low as in the dark open ocean, where the water temperatures are below 5 °C (Ma et al., 2023). The decomposition of vegetative cells in the diatom *Ditylum brightwellii* was shown to be decreased by lowering temperature from 15°C to 8°C, due to reduced respiration (Peters, 1996). Given the restricted energy supply under low O_2, the abilities

of vegetative diatoms to withstand acidic stress could be further dampened. The combination of colder (< 8°C) conditions and darkness was demonstrated to induce diatoms to form resting cells, including the diatom *T. pseudonana* used in the present work and other studies (Anderson, 1976; Chen et al., 2014). Recent research has indicated that the cellular energy supply plays crucial role in the transition of *T. pseudonana* from vegetive to resting stages in cold (5°C) and dark environments (Wang et al., 2024). Therefore, it is possible that progressive ocean deoxygenation in the open dark ocean would more likely induce settling diatoms to enter the resting stage.

The extensive sinking of algal cells following blooms may provide an opportunity for the microalgae to maintain their seed stock (Smetacek, 1985; McQuoid et al., 2002; McMinn and Martin, 2013). Notwithstanding, the intensifying hypoxia, marked by a decline in the pO_2 and an increase in the pCO_2, may pose a threat to the surviving strategy in view of the exacerbated impacts of the DeO_2 and OA on the diatoms during the darkness (this work). In the East China Sea near Changjiang estuary, surface diatom blooms strongly correlate with bottom hypoxia (Wang et al., 2017). The hypoxic layer in the bottom water is notably thick, expanding to a depth of 5 m below the sea surface and overlapping with the euphotic layer (Pei et al., 2009; Ye et al., 2016). Considering the sinking rates (~1.5 m d^{-1}) of diatoms (Riebesell, 1989), the time point during prolonged darkness can be mapped to depth. Based on this, our work could provide insights into the effects of the expanded hypoxic zone on the fate of diatoms as they descend from the euphotic layer in

coast waters (Figure 5). Even in oxygenated water column, *T. pseudonana* could culminate in ~57% biomass loss before settling to the seabed. However, under hypoxic conditions, the biomass of surviving *T. pseudonana* is expected to decrease by an additional 79%. In contrast, that of *T. weissflogii* suggests a 24% increase in hypoxic waters. Even when deposited in anoxic sediments, diatoms can extend their survival by utilizing nitrate respiration and undergoing dark fermentation (Kamp et al., 2011, 2013; Bourke et al., 2017). This increases the likelihood of their resuspension in a healthy cell form under the influence of both physical and biological factors, potentially serving as a source for the next growth cycle. This phenomenon has been confirmed in shallower coastal areas and freshwater lakes (Preston et al., 1980; Peipoch and Ensign, 2022). However, the divergent fate observed in the mass sinking process, coupled with the delayed recovery of biomass and photosynthetic performance, suggests that ocean deoxygenation could impede the contributions of resuspended phytoplankton to the restoration of primary production and the re-oxidation of infiltrated hypoxic water (Figure 5).

While our results are laboratory-based and do not necessarily directly extrapolate to natural coastal hypoxic environments, they do suggest that reduced O_2 levels weaken the ability of the *T. pseudonana* and *T. weissflogii* to withstand inherent acid stress from elevated CO_2. Considering ongoing ocean climate changes, including ocean acidification, ocean warming, and the production of H_2S under anoxic conditions, the imbalance between O_2 availability and metabolic O_2 demand may be exacerbated. Whether the observed effects are widespread among diatoms and
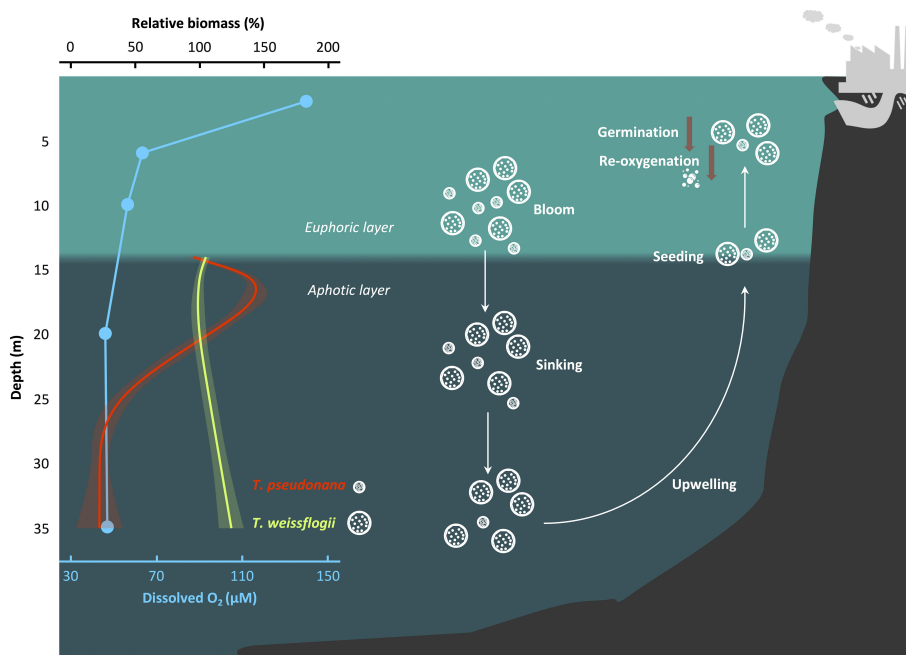

FIGURE 5

Scheme that illustrates the fate of diatoms as they sink into the hypoxic zone. The relative biomass is defined as $\frac{Cell_{LOHC} - \overline{Cell_{AOAC}}}{Cell_{AOAC}} * 100$. GAMs were constructed to analyze the changes in biomass of diatoms during the sinking process. The relationship between depth and biomass was derived from the relationship between time and cell concentration, utilizing an reported diatom sinking rate of 1.5 m d^{-1} (Riebesell, 1989). Solid lines and shadows are predicted values from GAMs with 95% confidence interval. Blue dots indicate the dissolved O_2 concentration in the hypoxic area of the East China Sea as recorded in August 2013 (Ye et al., 2016). The depth of the euphotic layer's bottom was calculated based on a report by Pei et al. (2009), which studied the same region and season. White and brown arrows indicate directions and decrease, respectively.

other phytoplankton taxa remains to be examined. Future studies are expected to quantify changes in respiratory energy production of various diatom species under varying O_2 levels and energy demands under different stressors to better understand the impact of ocean environmental changes on the "seed bank" of diatoms.

Data availability statement

The original contributions presented in the study are included in the article/Supplementary Material. Further inquiries can be directed to the corresponding author.

Author contributions

JS: Writing – original draft, Writing – review & editing, Formal analysis, Visualization, Funding acquisition. DZ: Writing – review & editing. XY: Writing – review & editing. JB: Writing – review & editing. KG: Writing – original draft, Writing – review & editing, Formal analysis, Funding acquisition.

Funding

Acknowledgments

Conflict of interest

The authors declare that the research was conducted in the absence of any commercial or financial relationships that could be construed as a potential conflict of interest.

Publisher's note

All claims expressed in this article are solely those of the authors and do not necessarily represent those of their affiliated organizations, or those of the publisher, the editors and the reviewers. Any product that may be evaluated in this article, or claim that may be made by its manufacturer, is not guaranteed or endorsed by the publisher.

Supplementary material

The Supplementary Material for this article can be found online at: https://www.frontiersin.org/articles/10.3389/fmars.2024.1387552/full#supplementary-material

References

Agusti, S., Gonzalez-Gordillo, J. I., Vaque, D., Estrada, M., Cerezo, M. I., Salazar, G., et al. (2015). Ubiquitous healthy diatoms in the deep sea confirm deep carbon injection by the biological pump. *Nat. Commun.* 6, 7608. doi: 10.1038/ncomms8608

Anderson, O. R. (1976). Respiration and photosynthesis during resting cell formation in *Amphora coffeaeformis* (Ag.) Kutz. *Limnol. Oceanogr.* 3, 452–456. doi: 10.4319/lo.1976.21.3.0452

Bai, X., Song, H., Lavoie, M., Zhu, K., Su, Y., Ye, H., et al. (2016). Proteomic analyses bring new insights into the effect of a dark stress on lipid biosynthesis in *Phaeodactylum tricornutum*. *Sci. Rep.* 6, 25494. doi: 10.1038/srep25494

Bienfang, P. K., Harrison, P. J., and Quarmby, L. M. (1982). Sinking rate response to depletion of nitrate, phosphate and silicate in four diatoms. *Mar. Biol.* 67, 295–302. doi: 10.1007/BF00397670

Bourke, M. F., Marriott, P. J., Glud, R. N., Hasler-Sheetal, H., Kamalanathan, M., Beardall, J., et al. (2017). Metabolism in anoxic permeable sediments is dominated by eukaryotic dark fermentation. *Nat. Geosci.* 10, 30–35. doi: 10.1038/ngeo2843

Breitburg, D., Levin, L. A., Oschlies, A., Gregoire, M., Chavez, F. P., Conley, D. J., et al. (2018). Declining oxygen in the global ocean and coastal waters. *Science* 359, eaam7240. doi: 10.1126/science.aam7240

Broman, E., Sachpazidou, V., Dopson, M., and Hylander, S. (2017). Diatoms dominate the eukaryotic metatranscriptome during spring in coastal 'dead zone' sediments. *Proc. Biol. Sci.* 284, 20171617. doi: 10.1098/rspb.2017.1617

Cai, W.-J., Hu, X., Huang, W.-J., Murrell, M. C., Lehrter, J. C., Lohrenz, S. E., et al. (2011). Acidification of subsurface coastal waters enhanced by eutrophication. *Nat. Geosci.* 4, 766–770. doi: 10.1038/ngeo1297

Chen, C., Li, Q., Zhou, Q., Sun, L., Zheng, M., and Gao, Y. (2014). Accumulation of free amino acid in the marine diatom resting cells during rejuvenation. *J. Sea. Res.* 85, 483–490. doi: 10.1016/j.seares.2013.08.003

Dehning, I., and Tilzer, M. M. (1989). Survival of *Schenedesmus aqumainatus* (Chlorophyceae) in darkness. *J. Phycol.* 25, 509–515. doi: 10.1111/j.1529-8817.1989.tb00256.x

Diaz, R. J., and Rosenberg, R. (2008). Spreading dead zones and consequences for marine ecosystems. *science* 321, 926–929. doi: 10.1126/science.1156401

Duarte, C. M., Losada, I. J., Hendriks, I. E., Mazarrasa, I., and Marbà, N. (2013). The role of coastal plant communities for climate change mitigation and adaptation. *Nat. Clim. Change* 3, 961–968. doi: 10.1038/nclimate1970

Eilers, P. H. C., and Peeters, J. C. H. (1988). A model for the relationship between light intensity and the rate of photosynthesis in phytoplankton. *Ecol. Modell.* 42, 199–215. doi: 10.1016/0304-3800(88)90057-9

Falkowski, P. G., and Raven, J. A. (1997). "Making cells," in *Aquatic photosynthesis, 2nd ed.* Eds. P. G. Falkowski. and J. A. Raven (Princeton University Press, Princeton), 278–318.

Franklin, D. J., Choi, C. J., Hughes, C., Malin, G., and Berges, J. A. (2009). Effect of dead phytoplankton cells on the apparent efficiency of photosystem II. *Mar. Ecol. Prog. Ser.* 382, 35–40. doi: 10.3354/meps07967

Gao, K., Beardall, J., Häder, D.-P., Hall-Spencer, J. M., Gao, G., and Hutchins, D. A. (2019). Effects of ocean acidification on marine photosynthetic organisms under the concurrent influences of warming, UV radiation, and deoxygenation. *Front. Mar. Sci.* 6. doi: 10.3389/fmars.2019.00322

Gao, K., and Campbell, D. A. (2014). Photophysiological responses of marine diatoms to elevated CO2 and decreased pH: a review. *Funct. Plant Biol.* 41, 449–459. doi: 10.1071/FP13247

Gao, K., Zhao, W., and Beardall, J. (2022). "Future responses of marine primary producers to environmental changes," in *Blue planet, red and green photosynthesis: Productivity and carbon cycling in aquatic ecosystems.* Eds. S. C. Maberly. and B. Gontero (ISTE Ltd and John Wiley & Sons, London and Hoboken), 273–304.

Gattuso, J.-P., Magnan, A., Billé, R., Cheung, W. W. L., Howes, E. L., Joos, F., et al. (2015). Contrasting futures for ocean and society from different anthropogenic CO_2 emissions scenarios. *Science* 349, aac4722. doi: 10.1126/science.aac4722

Gilbert, D., Rabalais, N. N., Díaz, R. J., and Zhang, J. (2010). Evidence for greater oxygen decline rates in the coastal ocean than in the open ocean. *Biogeosciences* 7, 2283–2296. doi: 10.5194/bg-7-2283-2010

Gobler, C. J., and Baumann, H. (2016). Hypoxia and acidification in ocean ecosystems: coupled dynamics and effects on marine life. *Biol. Lett.* 12, 20150976. doi: 10.1098/rsbl.2015.0976

Goldman, J. A., Bender, M. L., and Morel, F. M. (2017). The effects of pH and pCO_2 on photosynthesis and respiration in the diatom *Thalassiosira weissflogii*. *Photosynth. Res.* 132, 83–93. doi: 10.1007/s11120-016-0330-2

Hong, H., Li, D., Lin, W., Li, W., and Shi, D. (2017). Nitrogen nutritional condition affects the response of energy metabolism in diatoms to elevated carbon dioxide. *Mar. Ecol. Prog. Ser.* 567, 41–56. doi: 10.3354/meps12033

Jochem, F. J. (1999). Dark survival strategies in marine phytoplankton assessed by cytometric measurement of metabolic activity with fluorescein diacetate. *Mar. Bio.* 135, 721–728. doi: 10.1007/s002270050673

Juchem, D. P., Schimani, K., Holzinger, A., Permann, C., Abarca, N., Skibbe, O., et al. (2023). Lipid degradation and photosynthetic traits after prolonged darkness in four Antarctic benthic diatoms, including the newly described species *Planothidium wetzelii* sp. nov. *Front. Microbiol.* 14, 1241826. doi: 10.3389/fmicb.2023.1241826

Kamatani, O. O. A. (1997). Resting spore formation of the marine planktonic diatom *Chaetoceros anastomosans* induced by high salinity and nitrogen depletion. *Mar. Bio.* 127, 515–520. doi: 10.1007/s002270050040

Kamp, A., de Beer, D., Nitsch, J. L., Lavik, G., and Stief, P. (2011). Diatoms respire nitrate to survive dark and anoxic conditions. *Proc. Natl. Acad. Sci. U.S.A.* 108, 5649–5654. doi: 10.1073/pnas.1015744108

Kamp, A., Stief, P., Knappe, J., and de Beer, D. (2013). Response of the ubiquitous pelagic diatom *Thalassiosira weissflogii* to darkness and anoxia. *PloS One* 8, e82605. doi: 10.1371/journal.pone.0082605

Katayama, T., Murata, A., and Taguchi, S. (2011). Responses of pigment composition of the marine diatom *Thalassiosira weissflogii* to silicate availability during dark survival and recovery. *Plankton. Benthos. Res.* 6, 1–11. doi: 10.3800/pbr.6.1

Katayama, T., Murata, A., and Taguchi, S. (2015). Photosynthetic activation of the dark-acclimated diatom *Thalassiosira weissflogii* upon light exposure. *Plankton. Benthos. Res.* 10, 98–110. doi: 10.3800/pbr.10.98

Keeling, R. E., Kortzinger, A., and Gruber, N. (2010). Ocean deoxygenation in a warming world. *Ann. Rev. Mar. Sci.* 2, 199–229. doi: 10.1146/annurev.marine.010908.163855

Kennedy, F., Martin, A., Bowman, J. P., Wilson, R., and McMinn, A. (2019). Dark metabolism: a molecular insight into how the Antarctic sea-ice diatom *Fragilariopsis cylindrus* survives long-term darkness. *New Phytol.* 223, 675–691. doi: 10.1111/nph.15843

Lee, E., Ahn, H., and Choe, E. (2014). Effects of light and lipids on chlorophyll degradation. *Food Sci. Biotechnol.* 23, 1061–1065. doi: 10.1007/s10068-014-0145-x

Lewis, J., Harris, A., Jones, K., and Edmonds, R. (1999). Long-term survival of marine planktonic diatoms and dinoflagellates in stored sediment samples. *J. Plankton. Res.* 21, 343–354. doi: 10.1093/plankt/21.2.343

Li, F., Beardall, J., and Gao, K. (2018). Diatom performance in a future ocean: interactions between nitrogen limitation, temperature, and CO_2-induced seawater acidification. *ICES. J. Mar. Sci.* 75, 1451–1464. doi: 10.1093/icesjms/fsx239

Limburg, K. E., Breitburg, D., Swaney, D. P., and Jacinto, G. (2020). Ocean deoxygenation: A primer. *One Earth.* 2, 24–29. doi: 10.1016/j.oneear.2020.01.001

Ma, Z. P., Hu, Z. X., Deng, Y. Y., Shang, L. X., Gobler, C. J., and Tang, Y. Z. (2020). Laboratory culture-based characterization of the resting stage cells of the brown-tide-causing pelagophyte, *Aureococcus anophagefferens*. *J. Mar. Sci. Eng.* 8, 1027 doi: 10.3390/jmse8121027

Ma, J., Li, X., Song, J., Wen, L., Wang, Q., Xu, K., et al. (2023). The effects of seawater thermodynamic parameters on the oxygen minimum zone (OMZ) in the tropical western Pacific Ocean. *Mar. pollut.* 187, 114579. doi: 10.1016/j.marpolbul.2023.114579

Malone, T. C., Falkowski, P. G., Hopkins, T. S., Rowe, G. T., and Whitledge, T. E. (1983). Mesoscale response of diatom populations to a wind event in the plume of the Hudson River. *Deep. Sea. Res. Part I. Oceanogr. Res. Pap.* 30, 149–170. doi: 10.1016/0198-0149(83)90066-3

McMinn, A., and Martin, A. (2013). Dark survival in a warming world. *Proc. R. Soc B.* 280, 20122909. doi: 10.1098/rspb.2012.2909

McQuoid, M. R., and Godhe, A. (2004). Recruitment of coastal planktonic diatoms from benthic versus pelagic cells: Variations in bloom development and species composition. *Limnol. Oceanogr.* 49, 1123–1133. doi: 10.4319/lo.2004.49.4.1123

McQuoid, M. R., Godhe, A., and Nordberg, K. (2002). Viability of phytoplankton resting stages in the sediments of a coastal Swedish fjord. *Eur. J. Phycol.* 37, 191–201. doi: 10.1017/S0967026202003670

Mestre, M., and Hofer, J. (2021). The microbial conveyor belt: Connecting the globe through dispersion and dormancy. *Trends Microbiol.* 29, 482–492. doi: 10.1016/j.tim.2020.10.007

Millero, F. J., Graham, T. B., Huang, F., Bustos-Serrano, H., and Pierrot, D. (2006). Dissociation constants of carbonic acid in seawater as a function of salinity and temperature. *Mar. Chem.* 100, 80–94. doi: 10.1016/j.marchem.2005.12.001

Mock, T., Otillar, R. P., Strauss, J., McMullan, M., Paajanen, P., Schmutz, J., et al. (2017). Evolutionary genomics of the cold-adapted diatom *Fragilariopsis cylindrus*. *Nature* 541, 536–540. doi: 10.1038/nature20803

Mou, S., Zhang, Z., Zhao, H., Nair, S., Li, Y., Xu, K., et al. (2022). A dark-tolerant diatom (Chaetoceros) cultured from the deep sea. *J. Phycol.* 58, 208–218. doi: 10.1111/jpy.13240

Nymark, M., Valle, K. C., Hancke, K., Winge, P., Andresen, K., Johnsen, G., et al. (2013). Molecular and photosynthetic responses to prolonged darkness and subsequent acclimation to re-illumination in the diatom *Phaeodactylum tricornutum*. *PloS One* 8, e58722. doi: 10.1371/journal.pone.0058722

Oku, O., and Kamatani, A. (1999). Resting spore formation and biochemical composition of the marine planktonic diatom *Chaetoceros pseudocurvisetus* in culture: ecological significance of decreased nucleotide content and activation of the xanthophyll cycle by resting spore formation. *Mar. Biol.* 135, 425–436. doi: 10.1007/s002270050643

Pei, S., Shen, Z., and Laws, E. A. (2009). Nutrient dynamics in the upwelling area of Changjiang (Yangtze River) estuary. *J. Coast. Res.* 253, 569–580. doi: 10.2112/07-0948.1

Peipoch, M., and Ensign, S. H. (2022). Deciphering the origin of riverine phytoplankton using *in situ* chlorophyll sensors. *Limnol. Oceanogr. Lett.* 7, 159–166. doi: 10.1002/lol2.10240

Peters, E. (1996). Prolonged darkness and diatom mortality: II. Marine temperate species. *J. Exp. Mar. Biol. Ecol.* 207, 43–58. doi: 10.1016/0022-0981(95)02519-7

Pinheiro, J. C., and Bates, D. M. (2006). *Mixed-effects models in S and S-PLUS* (New York: Springer).

Preston, T., Stewart, W. D. P., and Reynolds, C. S. (1980). Bloom-forming cyanobacterium *Microcystis aeruginosa* overwinters on sediment surface. *Nature* 288, 365–367. doi: 10.1038/288365a0

Price, N. M., and Harrison, P. J. (1988). Uptake of urea C and urea N by the coastal marine diatom *Thalassiosira pseudonana*. *Limnol. Oceanogr.* 33, 528–537. doi: 10.4319/lo.1988.33.4.0528

Qu, L. M., Beardall, J., Jiang, X., and Gao, K. (2021). Elevated pCO_2 enhances under light but reduces in darkness the growth rate of a diatom, with implications for the fate of phytoplankton below the photic zone. *Limnol. Oceanogr.* 66, 3630–3642. doi: 10.1002/lno.11903

Raven, J. A., and Beardall, J. (2022). Evolution of phytoplankton in relation to their physiological traits. *J. Mar. Sci. Eng.* 10, 194. doi: 10.3390/jmse10020194

Riebesell, U. (1989). Comparison of sinking and sedimentation rate measurements in a diatom winter/spring bloom. *Mar. Ecol. Prog. Ser.* 54, 109–119. doi: 10.3354/meps054109

Ritchie, R. J. (2006). Consistent sets of spectrophotometric chlorophyll equations for acetone, methanol and ethanol solvents. *Photosyn. Res.* 89, 27–41. doi: 10.1007/s11120-006-9065-9

Schaub, I., Wagner, H., Graeve, M., and Karsten, U. (2017). Effects of prolonged darkness and temperature on the lipid metabolism in the benthic diatom *Navicula perminuta* from the Arctic Adventfjorden, Svalbard. *Polar. Biol.* 40, 1425–1439. doi: 10.1007/s00300-016-2067-y

Smetacek, V. S. (1985). Role of sinking in diatom life-history cycles: ecological, evolutionary and geological significance. *Mar. Biol.* 84, 239–251. doi: 10.1007/BF00392493

Strickland, J. D. H., and Parsons, T. R. (1968). A practical handbook of seawater analysis., (1968). *Bull. Fisheries. Res. Board. Canada.* 167, 49–80.

Sun, J.-Z., Wang, T., Huang, R., Yi, X., Zhang, D., Beardall, J., et al. (2022). Enhancement of diatom growth and phytoplankton productivity with reduced O_2 availability is moderated by rising CO_2. *Commun. Biol.* 5, 54. doi: 10.1038/s42003-022-03006-7

Sunda, W. G., Price, N. M., and Morel, F. M. M. (2005). "Trace metal ion buffers and their use in culture studies," in *Algal Culturing Techniques*, ed. Anderson, R. A. (Cambridge, MA: Elsevier Academic Press), 35–63.

Taylor, A. R., Brownlee, C., and Wheeler, G. L. (2012). Proton channels in algae: reasons to be excited. *Trends Plant Sci.* 17, 675–684. doi: 10.1016/j.tplants.2012.06.009

Wang, B., Chen, J., Jin, H., Li, H., Huang, D., and Cai, W. J. (2017). Diatom bloom-derived bottom water hypoxia off the Changjiang estuary, with and without typhoon influence. *Limnol. Oceanogr.* 62, 1552–1569. doi: 10.1002/lno.10517

Wang, G., Huang, L., Zhuang, S., Han, F., Huang, Q., Hao, M., et al. (2024). Resting cell formation in the marine diatom *Thalassiosira pseudonana*. *New. Phytol.* doi: 10.1111/nph.19646

Wong, J. C. Y., Raven, J. A., Aldunate, M., Silva, S., Gaitán-Espitia, J. D., Vargas, C. A., et al. (2023). Do phytoplankton require oxygen to survive? A hypothesis and model synthesis from oxygen minimum zones. *Limnol. Oceanogr.* 68, 1417–1437. doi: 10.1002/lno.12367

Wood, S. N. (2017). *Generalized additive models: an introduction with R* (Boca Raton: CRC press).

Wu, Y., Gao, K., and Riebesell, U. (2010). CO_2-induced seawater acidification affects physiological performance of the marine diatom *Phaeodactylum tricornutum*. *Biogeosciences* 7, 2915–2923. doi: 10.5194/bg-7-2915-2010

Ye, W., Zhang, G., Zhu, Z., Huang, D., Han, Y., Wang, L., et al. (2016). Methane distribution and sea-to-air flux in the East China Sea during the summer of 2013: Impact of hypoxia. *Deep. Sea. Res. Part II. Top. Stud. Oceanogr.* 124, 74–83. doi: 10.1016/j.dsr2.2015.01.008

Zuur, A. F., Ieno, E. N., Walker, N. J., Saveliev, A. A., and Smith, G. M. (2009). *Mixed effects models and extensions in ecology with R* (New York: Springer).